

General Disclaimer

One or more of the Following Statements may affect this Document

- This document has been reproduced from the best copy furnished by the organizational source. It is being released in the interest of making available as much information as possible.
- This document may contain data, which exceeds the sheet parameters. It was furnished in this condition by the organizational source and is the best copy available.
- This document may contain tone-on-tone or color graphs, charts and/or pictures, which have been reproduced in black and white.
- This document is paginated as submitted by the original source.
- Portions of this document are not fully legible due to the historical nature of some of the material. However, it is the best reproduction available from the original submission.

PRINCETON UNIVERSITY
Department of Astrophysical Sciences

FINAL REPORT
NSR 31-001-259

DEVELOPMENT AND EVALUATION OF INFRARED
SENSITIVE IMAGE SENSORS FOR SPACE ASTRONOMY

for

HEADQUARTERS
NATIONAL AERONAUTICS AND SPACE ADMINISTRATION
Washington, D.C.

May 5, 1975

PERSONNEL

Principal Investigator

Dr. Donald C. Morton

Technical Staff

John Lowrance
Donald Long
Patrick Murray
Manfred Rost
Andrew Siroki
Paul Zucchini

FISCAL STATUS

Value of Contract

\$89,423

Expenditures as of April 30, 1974

89,423

BALANCE

-0-

May 13, 1975



I. PURPOSE

Develop and evaluate infrared sensors for space astronomy.

II. ACTIVITIES

The program consisted of evaluating three sensors, a Xerox EOS vidicon, a RCA silicon vidicon and a General Electric doped germanium vidicon in a General Electric Camera.

A. Xerox EOS Vidicon Evaluation

An EOS model XV1010 developmental vidicon was operated in a cooled, slow scan, test set to evaluate its usefulness for exposure times in the range of 10 seconds and longer.

The data sheet indicated a dark current of 200 nanoamperes, at room temperature. Since that is four orders of magnitude too high for the proposed exposure times, cooling of the photoconductor is required. It was estimated that a temperature reduction of 100 to 130°C would suffice.

Test Results

Cooling the interior of the camera head (the immediate environment of the tube) to -130°C (measured 2 cm ahead of the target) was required to obtain marginal operation.

It was thought that the high power dissipation of the gun heater (6.3 volts, 300 ma, 3.8 watts) was preventing the target from becoming sufficiently cold. The heater voltage was reduced to two volts which reduced the heater power to 0.68 watts (339 ma) a reduction of 5.5 to one. The resulting cooling of the target separated the photoconductor from the conductive window coating in many stripes rather extensively damaging the target. Although cosmetically severe, the target damage did not prevent continued evaluation of the tube.

At the reduced heater operating level of 2 volts, the dark current at an ambient temperature of -77°C was in the order of 120 picoamperes at a target bias voltage of 8.2 volts. The dark current fluctuated over a 2 to 1 span as the cooling apparatus cycled in the order of 7°C.

Curve 2 of Figure 1 shows the transfer function obtained with an unfiltered incandescent light source. The incandescent source temperature was estimated to be in the order of 2200°K .

Curve 1 of Figure 1 shows the measured dark current under the operating conditions listed in Figure 1. Note the dark current is large compared with the signal current.

Figure 2 shows the severe effect of gun heater voltage on dark current.

Although detailed measurements of resolution were not made, the response to a square wave test pattern was found to be 50% at approximately 15 cycles per mm.

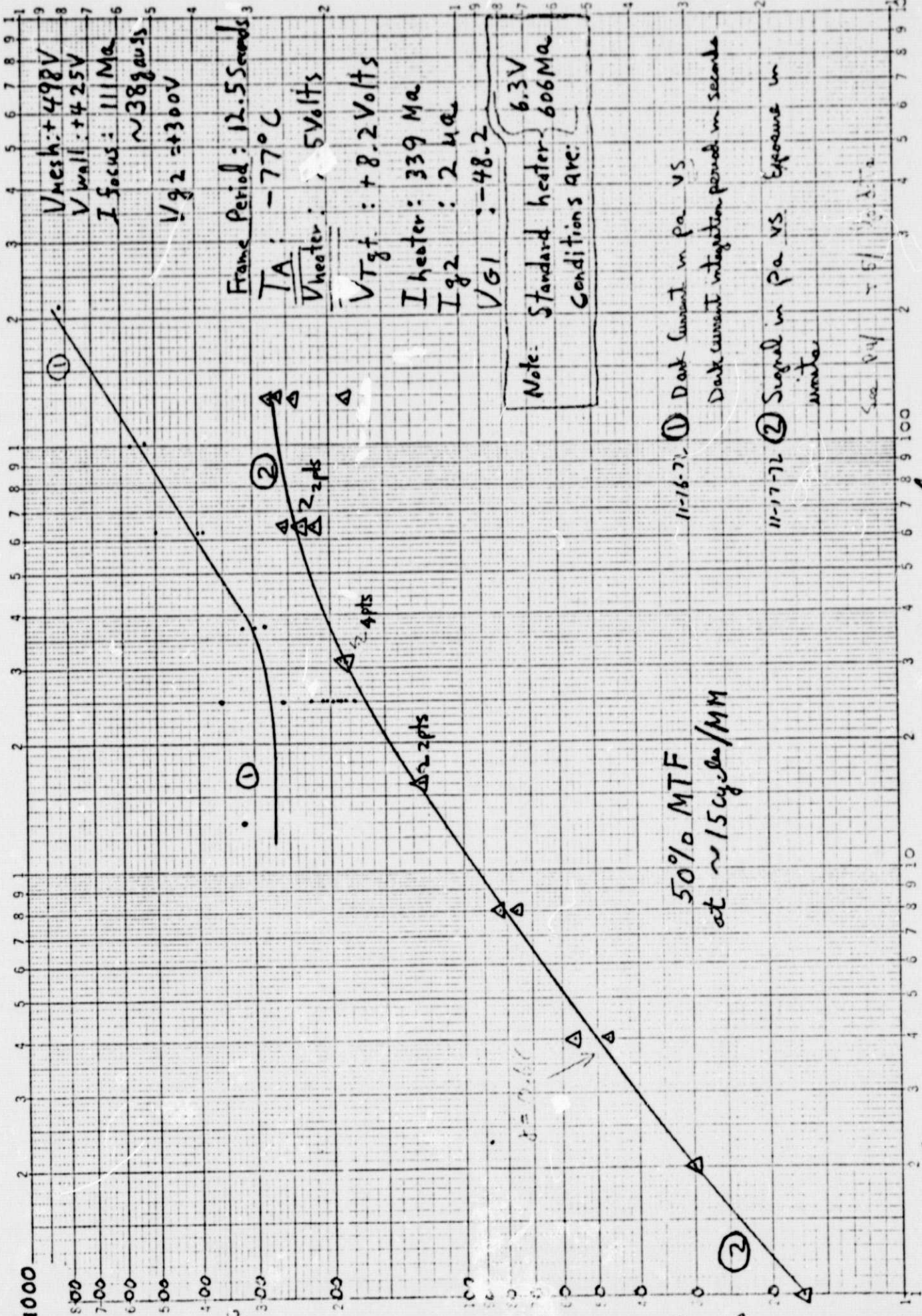
Very crude tests with 8000\AA and 7500\AA narrow band filters did confirm the tube's response to near infrared illumination.

Conclusions

Operation of infrared vidicons of this type for long exposures could be improved significantly if fitted with lower power electron gun heaters.

Photoconductors of comparable infrared response with lower dark currents would, of course, be helpful.

Eos Tube type 60-2-113-M
SN 7052369



EXPOSURE UNITS
Dark Current Integration Period, Seconds

Figure 1

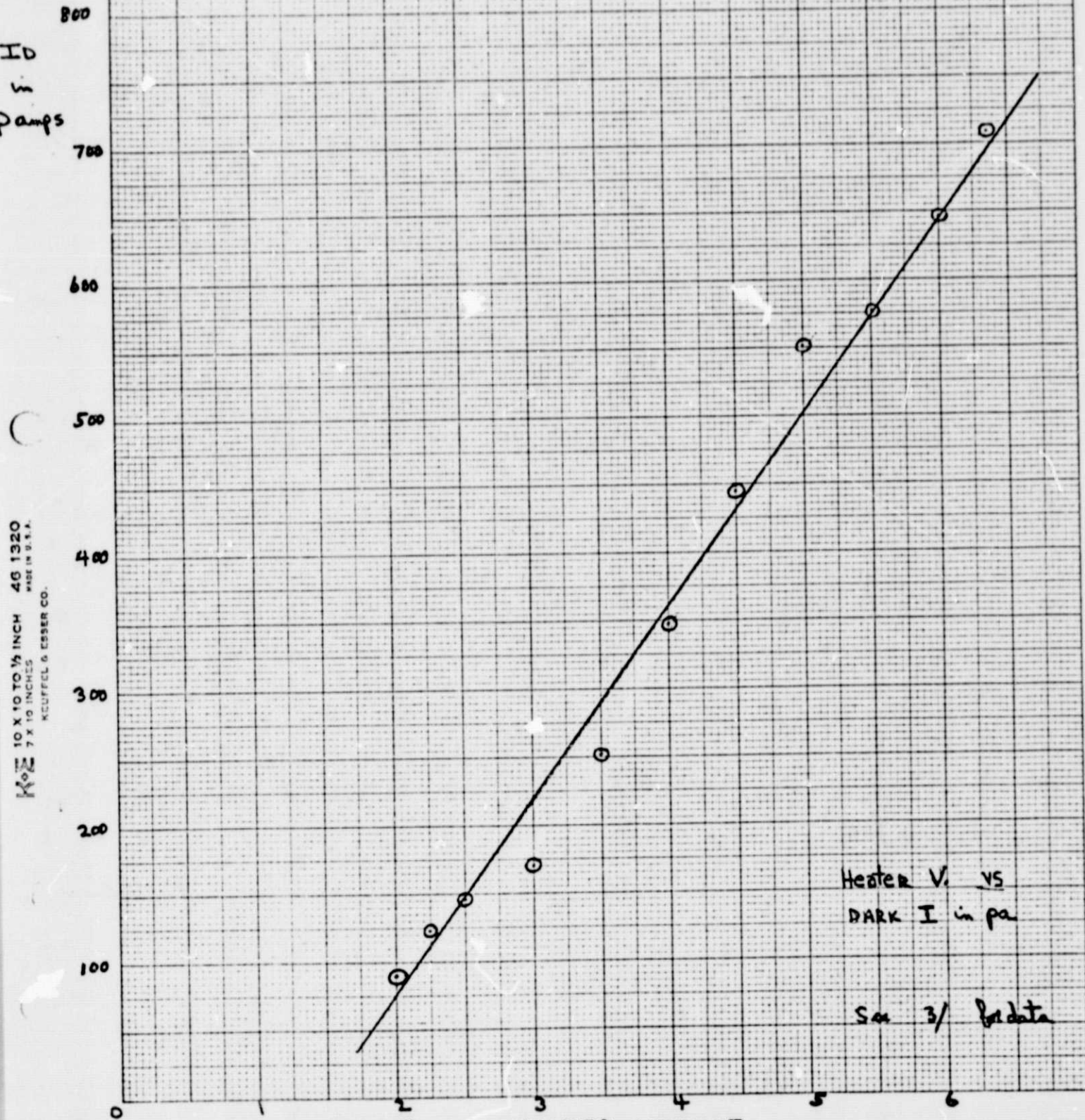
EOS Tube

Figure 2

Approx. TA: -70°C

$V_T = 8.1\text{V}$

$I_b = 7.2\text{mA}$



Hester V. vs
DARK I in pA

See 3/1 data

Model 10 X 10 TO 1/2 INCH 46 1320
MADE IN U.S.A.
KEUFFEL & ESSER CO.

B. RCA Silicon Vidicon Evaluation

An RCA 3585 silicon vidicon with an enhanced red response was tested in the laboratory for IR sensitivity, frequency response, noise and integrating capabilities. The results of this study are reported in the following report by Crane and Davis, which was published in "Publications of the Astronomical Society of the Pacific", February 1975.

CHARACTERISTICS OF THE SILICON DIODE VIDICON

PHILIPPE CRANE AND MARC DAVIS

Joseph Henry Laboratories, Physics Department, Princeton University

Received 1974 July 22, revised 1974 October 4

A series of laboratory tests of the silicon diode vidicon has yielded valuable information of particular importance to astronomers. The vidicons were operated in slow-scan mode. The tests showed that these vidicons can be expected to operate with a dynamic range of 1000, a signal-to-noise ratio of 200:1, an MTF of 50% at 10 cycles mm^{-1} , and integration capabilities of several hours. The noise in the output does not appear to be limited by photon statistics, but is dominated by systematic effects. The results confirm that these devices are extremely good sensors for low-contrast high-optical flux problems in astronomy.

Key words: instrumentation — photometry

1. Introduction

The silicon diode vidicon has many attractive features for certain types of astronomical observations. Among these are: high-quantum efficiency over most of the visible spectral range including exceptionally good response in the wavelength region from 6000 Å to 10,000 Å, an extremely large dynamic range, and an almost linear photometric response. Cooling the tubes to about -60°C allows integration times on the order of several hours with relatively little loss in dynamic range due to leakage current. However, there are some sacrifices that must be weighed with the above advantages in planning an application of these devices. Generally, the spatial resolution that can be obtained with currently available silicon diode targets is not as great as can be obtained with certain other targets and sensors. Also, since each incident photon produces at most one charge-hole pair, and since this pair leaves a change of only one charge on the diode matrix as evidence of the photon, the minimum detectable number of incident photons is in principle limited by the noise in the first stage of the preamplifier. This noise is typically on the order of several hundred electrons per resolution element and implies that this type of vidicon will not be useful in applications where the number of photons is small. The great advantages of the silicon diode tube are realized in observational programs where there is a relatively high flux of photons per picture element and it is desired to make exposures which attain an extremely high signal-to-noise

ratio. The high signal-to-noise ratio can be obtained since the large dynamic range allows many tens of thousands of photon events per resolution element to be accumulated and hence good statistical precision to be achieved.

An important problem for the application of these devices is to understand the extent to which the above inherent capabilities of these tubes can be realized in actual astronomical observations. It is the purpose of this paper to report on a laboratory evaluation of some of the relevant characteristics of the silicon vidicon. The main emphasis of this work has been to attempt to understand the sources of noise in the video output, and the extent to which the video signal can be considered photon noise limited.

There have been several previous papers dealing with various properties of silicon diode vidicons. One of the earliest and most-comprehensive papers is the work of Crowell and Labuda (1969) dealing with physical properties of the silicon target. More recent work, more along the lines of application to astronomical problems, are the papers by McCord and Westphal (1972) and by McCord and Bosel (1973) which touch on some aspects of the problems discussed here. There are, of course, many other papers in the literature dealing with various aspects of the silicon vidicon, but a full review of the literature is not appropriate here.

Section II below discusses the details of the electronic hardware employed in this study. Section III discusses the various tests that were performed, but a full discussion of the noise is

reserved for Section IV. Section V makes some quantitative evaluations of the observational possibilities. Section VI summarizes our results.

II. Camera-System Details

The camera system that was used in this work is the same one that has been employed by Lowrance and Zucchini (1974) for the development of the SEC Vidicon tube. The sweep generators, sweep amplifiers, the synch generator, and various control circuits of the SEC system were modified slightly to allow them to drive the silicon diode tube. The only piece of new construction that was required was a new camera head. Figure 1 shows a block diagram of the camera system and indicates some of the functions of the various parts. The paragraphs below describe some of the relevant details of the hardware.

A. Camera Head

The camera head consisted of: the silicon diode vidicon tube, the focus and deflection coil assembly, a liquid-nitrogen-cooled cold box, the initial preamplifier, and some other associated devices such as erase lamps that were used to short-circuit the diodes prior to a recharging cycle. The cold box, a Products for Research Model TE-114V, had the capability of cooling the tube to well below -100°C , but was normally operated at about -60°C since the dark current in the tube was sufficiently low at this temperature to allow several hours of integra-

tion. The first stage of the preamplifier was mounted inside the cold box in as close proximity to the target flange as possible in order to reduce the input capacitance and thus to reduce the noise associated with this capacitance. Another advantage in mounting the first stage in the cold box arose because of the reduction in the Johnson noise in the target-biasing resistor. The final operating condition of the preamplifier under these conditions gave a noise of about ± 400 electrons per resolution element. This figure probably could have been improved considerably, but would not have improved the tube threshold substantially since this was not the limiting element, as our discussion below points out.

The vidicon tubes that were used in this work were commercially available models manufactured by RCA. Three tubes were available for the tests described here. Two of these did not have a filament light shield and thus could not be used in the slow-scan mode because backlighting from the filament was too severe. The one tube which did have a filament light shield had reduced backlighting problems but nevertheless this remained a serious problem as the discussion in section V below indicates. The tube which was used for most of this work was an RCA 35S5 which had a nominal target thickness of 20μ and hence enhanced red response.

The sweep coil employed, an RCA C23230, is also commercially available.

B. Electronics and Control Circuitry

The electronic control system was extremely flexible; the target bias, the mesh potential, the wall-focus voltage, the scan size and position, the beam current, as well as many other parameters could be monitored and adjusted quite easily in order to optimize the performance of the camera. The number of scan lines per frame and the number of samples per scan line were also adjustable. It was important to set the number of scan lines in order to obtain a minimum of overlap between lines so that the vertical resolution would not be degraded. The number of points at which the individual scan lines were sampled was chosen so that the sampling frequency was just twice the frequency at which the minimum noise in the preamplifier occurred. This assured that the highest spatial frequencies of interest would

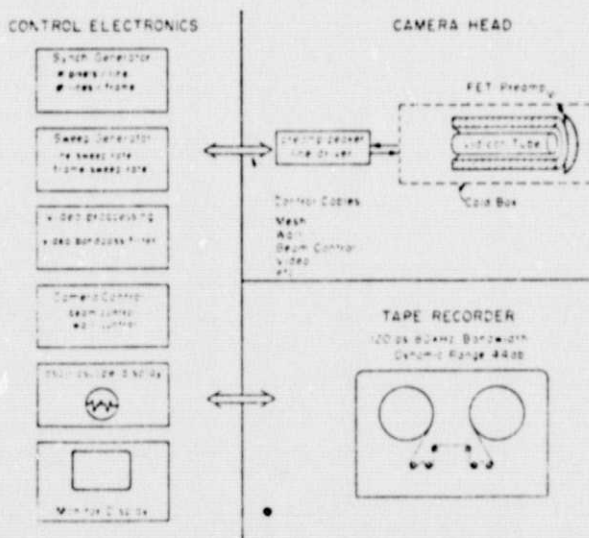


FIG. 1 — Block diagram of the camera system.

have as little extra noise from the preamplifier system as possible.

Following the initial preamplifier stage was a low-pass video filter. The rolloff frequency of this filter was chosen to suppress spatial frequencies which had been attenuated by more than 50% in the target and reading section. The digital sampling frequency was chosen to be 60 KHz, and the video filter frequency began to roll off at 20 KHz at a rate of about 40 db/octave. In our final configuration, we sampled 1024 points per scan line with 350 scan lines on the 1 cm² target area. During processing, the data were binned to 256 points per scan line thus defining a resolution element of approximately $30\ \mu \times 40\ \mu$.

An extremely important aspect of the controlling electronics is the stability, linearity, and reproducibility of the horizontal and vertical sweep circuits. The detailed reasons for this are discussed in section IV below. For our system, the generated sweep voltages were linear functions of the time to better than 0.05%. However, it is possible that the sweep coil and the history of the shielding of the sweep coil could have introduced larger time-dependent nonlinearities. The sweep circuits were stable and reproducible to better than 0.1%. This implies that the sweep circuitry could reliably place the electron beam to better than $10\ \mu$ on the target. These uncertainties in the beam position could well have been the limiting noise factor in this work (Westphal 1974).

Table I summarizes the various operating parameters of the system.

C. Operating Details

This section discusses some of the considera-

tions that governed the selection of various operating procedures and parameters. Most of this information does not reveal anything new about the silicon diode tube, but it is important that these procedures be described so that any systematic effects in our results can be evaluated by other workers.

Before making an exposure with the vidicon, it was necessary to prepare the target to a standard charge state. This was done by flooding the target with light from a set of light-emitting diodes, and then recharging through a fixed number of scan frames at the usual 6 seconds per frame rate. The exact number of frames did not matter critically past six, but was always constant within any particular set of data. During an exposure the filament was turned off and photons were accumulated on the target. Prior to the readout of an exposure, the filament was turned on and the target bias was raised by one-half volt in order to insure that the scanning beam would land efficiently even on areas of the target which had received little or no light. The reading-beam current was set at the point where further increases in this current did not increase the video signal. The first scan efficiency of the tubes was about 75% under these operating conditions, and although this was certainly not ideal, it was deemed adequate.

A rather serious problem with beam pulling near bright-point objects was noticed in these tubes. This occurs when the electron scanning beam passes near a highly exposed region of the target and is deflected from its usual path and incorrectly indicates the presence of light. Part of the reason for this phenomenon is that the focus field is only about 40 gauss and thus the scanning beam is not as stiff as it could be. One obvious way to reduce this problem is to increase the focus field strength. Although this problem was quite obvious and troublesome with our silicon diode tubes it is probably present but so far undetected in other vidicon detectors, and may represent a fundamental limitation to their use for certain astronomical problems.

III. Laboratory Evaluation

The laboratory-evaluation program covered a wide range of vidicon operational characteristics. These areas were the following: integration time versus temperature, spatial resolution, quantum

TABLE I

PARAMETERS OF A SINGLE SLOW SCAN FRAME

Scan size	1 cm \times 1 cm
Pixel time	16.2 μ sec/pixel
Line time	16.7 m sec/line
Frame time	5.9 sec/frame
Pixels/Line	1024
Resolution element	4 pixels summed together ($40\ \mu \times 30\ \mu$)
Lines/Frame	350
Scanning-beam spot size	$\sim 30\ \mu$

By far the most serious source of random noise in our system was the beam-switching noise which is generated when the hot electron beam recharges the back plate of the target to its equilibrium potential. Local thermodynamic equilibrium between the electron beam and the target implies an uncertainty in the charge transferred to the target given by the relation

$$\frac{(\Delta Q)^2}{2C} = \frac{1}{2} kT,$$

where T is the electron beam temperature ($\sim 1100^\circ \text{K}$) and C is the target capacitance per resolution element. Since, in practice, the target is prepared and then read out by the same scanning beam, there is an increased uncertainty from this mechanism due to the uncertainty in the initial charge state of the target. Thus the total uncertainty due to the scanning beam is given by

$$\Delta Q = \sqrt{2kTC}$$

The beam-switching noise was measured by repeatedly preparing and scanning the target and then examining the frame-to-frame fluctuations of the individual pixels. The output signal included the preamplifier noise as well but this was assumed to add in quadrature with the beam-switching noise, and could therefore be removed. Any additional noise introduced by the preparation procedures would have appeared as beam-switching noise in our procedure. A beam-switching noise of approximately 300 electrons per resolution element had been expected, but the measured value was close to 700 electrons per resolution element. One plausible explanation for part of this increased noise is that the electron beam striking the target is effectively much hotter than the 1100°K cathode.

Additional beam-switching noise may arise because the targets are discrete structures containing diodes spaced about 15μ apart. The scanning electron beam typically has a diameter of about 30μ and thus scans only a few diodes at a time, interacting with the diodes and the insulating regions between the diodes in a rather complex manner. It is also possible for this insulating region between the diodes to become charged causing nonrepeatable irregularities in the landing of the electron beam. Both of these mechanisms are possible causes for the increased beam-switching noise observed in our data. It

should be possible to reduce or eliminate beam-switching noise by introducing a cold cathode gun into the tube.

Photon-shot noise in the incident light beam was the source of noise which we wanted to measure most carefully. This noise should increase like the square root of the number of photons stored, and, therefore, we made exposures of different total intensity in order to measure the increased noise with increasing signal. The target was uniformly illuminated by a relatively cold incandescent bulb through a small, distant pinhole. Figure 2 is a graph of the results. Each measured point in this figure represents the fluctuations of individual picture elements about their mean value for several successive scans of the target at the same exposure level. The results indicate that our dominant noise source was a linear function of the exposure level, and that this noise completely dominated the expected photon-shot noise. An explanation for this is discussed below. In spite of the above limitations, the signal-to-noise ratio in the data was very good. For example, in an exposure of 6×10^5 electrons/resolution element, we measured a noise of 2200 electrons, thus giving a S/N of greater than 200:1.

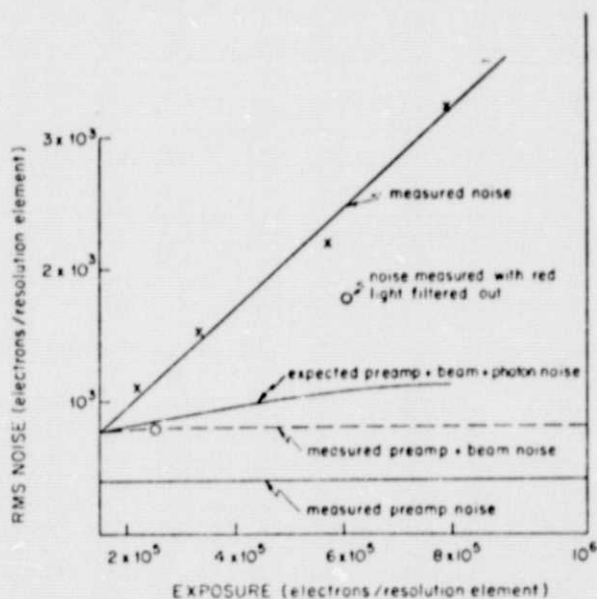


FIG. 2—Plot of noise versus exposure levels. The horizontal lines are the threshold levels for preamp noise and preamp and beam noise. Also shown are the expected and measured noise. The open circles are the measured noise with the red light ($\lambda > 9000 \text{ \AA}$) filtered out.

B. Sources of Nonrandom Noise

The main source of noise in our exposures has been determined to be a systematic error arising from micro-misregistration of the scanning electron beam with respect to the target. This misregistration can be an error in the initial positioning of the beam on the target, or it can be a non-repeatability of the scan. If the target is uniform and uniformly exposed, the first effect will not introduce any noise into the video signal. The second effect is a beam wandering phenomenon, in which the scanning beam can wander either perpendicular or parallel to the direction of travel. Evidence for both types of beam wander were found.

The silicon diode targets are not uniform and have significant sensitivity variations, which makes micro-misregistration a very serious noise source. In the presence of sensitivity variations, the linear noise term in Figure 2 is not unexpected because it is impossible to register the electron beam in a perfectly repeatable manner. Suppose that two frames are to be compared and that one frame is misregistered with respect to the other by ϵ . If $R(x)$ is the response of the target at position x , then the misregistration will produce a noise component with variance σ^2 given by

$$\sigma^2 = \left\langle \left(\frac{dR}{dx} \right)^2 \right\rangle \epsilon^2$$

Since R typically varies by $\sim 10\%$ in 100 microns when the target is illuminated by broadband red light in the 0.6-1.2 micron range, a 1% error can result if ϵ is of the order of 10μ , or one pixel. Furthermore, this noise component will grow linearly with the exposure.

The beam-wandering effects and registration errors could be somewhat reduced with a stiffer electron beam, but the greatest improvement would come if the targets could be made more uniform. The chief source of target nonuniformity arises from a Fabry-Perot interference within the silicon diode target. This occurs at the red end of the spectral sensitivity range where the target becomes transparent to the incident photons (Title 1974). Because silicon has a high index of refraction, there is significant reflection at the target boundaries causing standing waves to be set up within the target. If the targets were uniformly thick the spectral sensitivity would

vary periodically with wavelength. However, the targets are not uniformly thick, with variations of a few percent being common, and this gives rise to a microstructure of interference fringes. This microstructure appears as sensitivity variations across the target which change with wavelength. For illumination with a narrow spectral bandwidth, Title reports observing sensitivity variations greater than 100%. These interference fringes are not totally washed out even for broadband illumination in the red end of the sensitivity range since the reddest photons contribute relatively more strongly to the interference. The wavelength at which the interference effects become serious depends on the thickness of the target and the particular application under consideration.

Figure 3 shows an example of the type of interference that can be produced when the silicon target is uniformly illuminated by a pinhole light source using a relatively cold incandescent filament. This picture has had the low spatial frequencies filtered out in order to produce a constant background level in the reproduction. The mottling over the entire picture is quite reproducible from frame to frame. This reproducibility is shown in Figure 4 where the two upper traces are the same scan line from different TV frames, and the repeated pattern is obvious. The rms fluctuations of the upper traces in Figure 4 are about 6% of the video signal level. We have determined that these fluctuations remain a constant fraction of the signal level at all but the very lowest exposures and can thus be considered to be equivalent to variations in quantum efficiency.

The bottom trace in Figure 4 is the difference of the upper two and shows almost perfect elimination of the Fabry-Perot type microstructure. The remaining fluctuations in the difference of the two lines is a measure of the actual noise in the system. It is these rms fluctuations of several frames about their mean that have been plotted as the top line of Figure 2.

The scale size of the microstructure was determined by cross-correlation analysis of the uniform exposures, which indicated that the correlation length of the microstructure was of the order of 100μ to 200μ , while the correlation length of the difference of two properly registered frames was 40μ to 60μ , or about the same as the

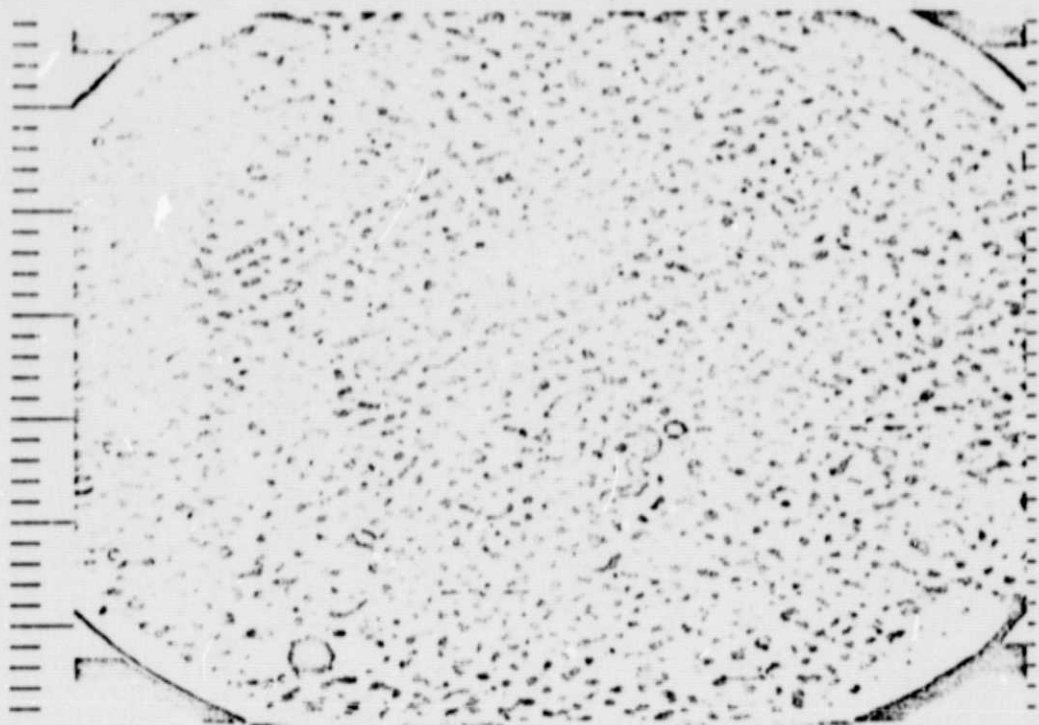


FIG. 3—High-contrast picture of target microstructure taken under uniform illumination with a cold incandescent filament. The small black-and-white regions are target blemishes. The notching is the Fabry-Perot target interference.

resolution limit of the target.

All frames used to compute the noise of Figure 2 were registered to within one pixel (10μ). It is apparent that the microstructure has not been completely eliminated, and that the resulting noise level is two to three times the "expected" noise level. Attempts to register frames to fractions of a pixel can make some further improvement, but the registration error was not found to be consistent for all segments of the target, and could fluctuate by $\sim \frac{1}{2}$ pixel within a single scan line. Noise fluctuations in the electron beam sweep rate of a few parts in 10^3 can easily account for this.

Spatial Fourier analysis of single scan lines, and of the difference of scan lines between frames indicates a reasonably flat power spectrum between 2 and 10 mm^{-1} , but there was significant $1/f$ noise up to spatial frequencies of 2 mm^{-1} . This could be caused by vertical oscillations of the horizontally scanning electron beam; the oscillations could be induced by instabilities in the vertical sweep amplifiers. This effect is apparent in the bottom trace of

Figure 4, where the baseline is slightly peaked in the center. The effect is of the order of $1\% - 2\%$, which could easily be generated by 1μ vertical



FIG. 4—Oscilloscope tracings of portions of the same line from two different frames. The bottom line is the difference of the top two and indicates the repeatability of the microstructure. The exposure level was 6×10^5 electrons/resolution element where the resolution element as defined in the text is the sum of four dots in the figure.

oscillations of the electron beam.

By placing a piece of ground glass, which absorbs light of wavelength greater than 9000 \AA , between the light source and the vidicon, we were able to substantially reduce the microstructure in our $20\text{-}\mu$ -thick target. We again measured the fluctuations between identical exposures, and these results are also shown in Figure 2. The noise level is significantly reduced, but still well above the photon-shot noise level.

To minimize difficulties with the microstructure of these targets, we would suggest filtering out light of wavelength larger than 9000 \AA in the $20\text{-}\mu$ targets and 7000 \AA in the $10\text{-}\mu$ targets. Title (1974) has suggested the targets be coated with an antireflective layer to reduce the interference effect. Recently several manufacturers have announced a photoconductive vidicon with quantum efficiency greater than 50% out to 8600 \AA . Many of the problems we encountered with the silicon diode vidicon should not be present with these tubes because their spatial structure is uniform.

V. Observational Implications

This section discusses some of the observational applications and constraints that would be influenced by the discussions in the previous sections. The relatively high threshold noise of the silicon vidicon implies that it will be extremely difficult if not impossible to use it for deep sky observations. For example, suppose one desired to detect point sources with a surface brightness of one percent of the night-sky background. The minimum signal-to-noise ratio per picture element would then have to be 100:1. At a dark site such as Kitt Peak, the sky brightness incident on the vidicon in the band between 7000 \AA – 8000 \AA would be of the order of $1.5 \times 10^7 f^{-2}$ photons $\text{cm}^{-2} \text{ sec}^{-1}$, where f is the focal ratio of the telescope in use (Broadfoot and Kendall 1968).

From Figure 2, we see that if we collect 2×10^5 electrons/resolution element ($40\text{-}\mu \times 30\text{-}\mu$) we will achieve a S/N of greater than 100. If the overall quantum efficiency of the system is ϵ (optimistically ~ 0.5) the integration time required is $10^5 f^2 \epsilon^{-1}$ seconds. Even on a fast optical system ($f \sim 3$), the integration time would be of the order of six hours, which is totally unreasonable. The threshold noise of the sili-

con diode vidicons is about four times higher than we had anticipated it would be, and is a major drawback to the use of silicon diode vidicons. Restating the situation, the high threshold noise implies that the S/N grows linearly with signal until the signal level is greater than 10^{-5} electrons/resolution element.

Another serious problem in doing photometry of very faint objects is to eliminate or to control the backlighting of the target from the electron beam cathode. Light from the hot filament can leak through the exit aperture of the electron gun, and strike the backside of the silicon. Even with the filament current turned down quite low, in an integration time of one minute, we could see an obvious bulls-eye pattern caused by filament backlighting of the target.

During long astronomical exposures it is essential that the filament be off. In order to establish the zero sky-exposure level of the target, it is also essential for the filament to be on for a definite, repeatable time interval during the readout and preparation procedure. A good way to do this would be for the filament to be turned off automatically at the end of the preparation process, and for the readout process to occur automatically after a fixed time interval from when the filament is turned back on. This type of procedure has been used by McCord and Bosel (1973), but the filament control was manually operated in our system.

VI. Conclusions

The quantitative evaluation of the silicon diode vidicon presented here has demonstrated the feasibility of using these devices for high-precision, high-flux, broadband astronomical problems. We have shown that a dynamic range of at least 1000 can be expected, that signal-to-noise ratios of 200:1 are easily obtained, and that a spatial resolution of 50% contrast at 10 cycles mm^{-1} can be achieved. Cooling the tubes to -60° C reduces the leakage current in the targets to a low enough level to allow several hours of integration with no appreciable loss of dynamic range.

In spite of the rather promising results mentioned above, there are some problems which must be considered in any application of the silicon diode vidicon. The problems of Fabry-Perot interference within the target cannot be

disregarded, and unless there are major changes in the manufacturing techniques, this will remain a problem. Beam-switching noise presently limits the threshold of the tubes and will also require manufacturing changes if it is to be eliminated. The problems associated with the discrete structure of the target can be reduced by employing more-stable and reproducible electron beam optics and targets with closer packed diodes, but the discrete structure problem will probably continue to be a limitation on the ability of these devices to achieve quantum noise limit operation over their full dynamic range. In addition, attempts to improve the spatial resolution will aggravate these problems.

In summary, the various advantages and disadvantages of the silicon diode vidicon should be carefully considered before the decision to use one of these devices is made. In many instances, the great advantages will far outweigh the limitations, and the silicon vidicon can be used efficiently to yield important new scientific results.

-- There are many people who have contributed to this work, John Lowrance and Paul Zucchini of the Astrophysical Sciences Department at Princeton have been extremely helpful and gen-

erous in lending equipment and advice. John Mon constructed the camera head and assisted in some of the early measurements. Eugene Gordon of Bell Telephone Laboratories, Murray Hill, made several helpful suggestions. One of us (P.C.) enjoyed the hospitality of the Aspen Center for Physics where portions of this work were completed.

REFERENCES

- Broadfoot, A. L., and Kendall, K. R. 1968, *J. Geophys. Res.* **73**, 426.
- Crane, P. 1973 in *Astronomical Observations with Television-Type Sensors*, J. W. Glaspey and G. A. H. Walker, eds. (Vancouver, B.C.: University of British Columbia), p. 391.
- Crowell, M. H., and Labuda, E. F. 1969, *Bell System Technical Journal* **48**, 1481.
- Lowrance, J. L., and Zucchini, P. 1974 in *Methods of Experimental Physics*, Vol. 12, Part A, N. Carleton, ed. (New York: Academic Press), p. 277.
- McCord, T. R., and Bosel, J. 1973 in *Astronomical Observations with Television-Type Sensors*, J. W. Glaspey and G. A. H. Walker, eds. (Vancouver, B.C.), p. 137.
- McCord, T. R., and Westphal, J. A. 1972, *Applied Optics* **11**, 522.
- Title, Alan 1974, *Solar Physics* **35**, 233.
- Westphal, J. A. 1974 (private communication).

C. General Electric IR Vidicon and General Electric Camera Electronics Evaluation

A GE Z-7934 Type vidicon which was mounted in a GE furnished cooled camera head was studied.

The GE camera operated at 30 frames/sec with 2:1 interlace readout and had the capability of adjustable integration period. Tests were run with integrations up to 10 minutes.

The GE camera was tested on the 36" Princeton telescope with observation of Jupiter, Mars, and Mira. The sources were detectable but S/N was poor even with long integration.

Additional laboratory evaluation determined that the threshold signal for the GE system was $5.6 \times 10^{-7} \text{ w/cm}^2$ at 2.5 microns with a bandwidth of 0.15 microns. This threshold proved to be too high to justify any additional scientific observations.